Supporting information for: Arbitrary waveform modulated pulse EPR at 200 GHz

Ilia Kaminker,[1] Ryan Barnes[1] and Songi Han[1,2]

1. Department of Chemistry and Biochemistry and 2. Department of Chemical Engineering University of California Santa Barbara.

Estimation of ω_1 inhomogeneity for BDPA in o-terphenyl sample from nutation and inversion data.

For a large sample that is larger than the wavelength we expect high inhomogeneity of the oscillating 200GHz magnetic field. In our setup a Teflon "bucket" filled with the sample of interest (BDPA in o-terphenyl powder) is positioned on top of the mirror at the bottom of the EPR probe. The height of the sample (5mm) exceeds the wavelength (~1.5mm) and we expect significant distribution in the strength of the oscillating magnetic field (ω_1) at different positions along the sample.

Standard procedure to determine the distribution of ω_1 is from an echo detected nutation curve data; the pulse sequence is shown on figure (S1a). In this experiment the frequency of the observed oscillations correspond to the central ω_1 frequency and the distribution can be deduced from the decay of these oscillations. In our case due to limited microwave power and correspondingly long pulses the decay associated with the T_2 decay (T_m = 3.3 µs) is of the same order of magnitude as the one caused by the ω_1 inhomogeneity. We therefore used simulations to find the best agreement between the simulated and experimental profiles. The simulations were based on a single, on-resonance, S=1/2 spin and included ω_1 distribution, experimentally determined T_1 and T_m relaxation rates. To account for the differences in bandwidth between the long inversion and shorter detection pulses only the side of the echo (725ns after the echo maximum) was integrated over width of 50ns. Integration window is illustrated as a grey rectangle on figure S1a. We find the best agreement between the experimental and simulated curve for ω_1 distribution represented as a Gaussian with a maximum of 0.35MHz and full width half maximum of 0.3MHz (figure S1b). Comparison of an experimental and simulated inversion profiles of a 1 µs long rectangular pulse using the ω_1 distribution determined from the nutation experiments is shown on figure S1c and the two are found to be in good agreement. Note that for the inversion profile simulation an EPR linewidth was included in the simulation as detailed in section "Theoretical model" in the SI.

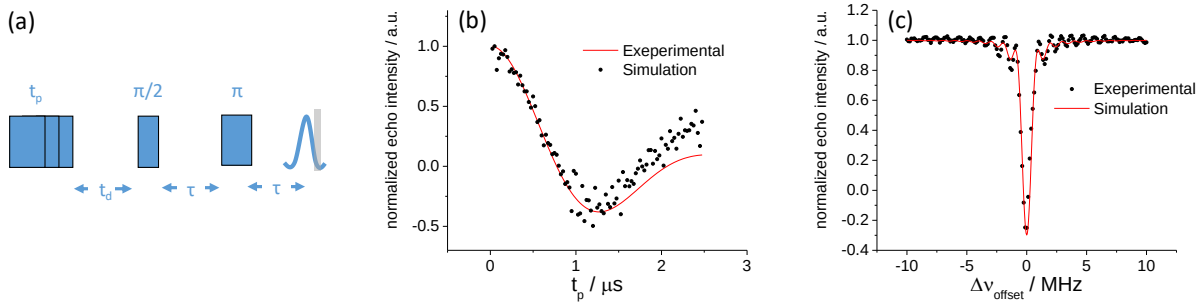

Figure S1. Nutation pulse sequence (a). Comparison between experimental and simulated nutation curves. (b) Comparison between experimental and simulated inversion profiles (c). Simulation parameters. T_2=3.3 µs; T_1 = 260 µs; ω_1 = 0.35MHz with

FWHM 0.3MHz; Experimental parameters: nutation experiment: BDPA (1% w/w) in o-terphenyl at room temperature. Frequency 197.589 GHz;; two step phase cycle. Experimental parameters inversion profile: Frequency 197.589 GHz; π/2 / π = 500 ns / 1 µs; τ = 1.1 µs; td = 2us, t_p = 1 µs;

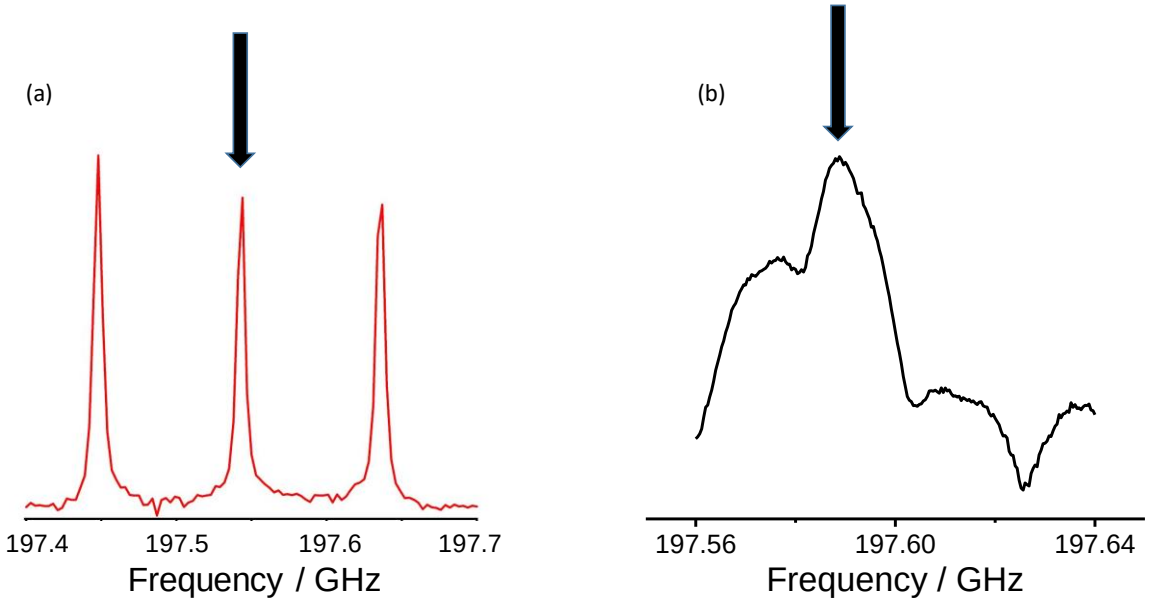

Figure S2. 200GHz frequency swept EPR spectra of Diamond (a) and 1% BDPA in o-terphenyl (b). Arrows point to the field positions where the experiments, presented in the main text, were performed. Note that the spectra are significantly distorted due to \convolution with a standing wave pattern of the bridge / probe, as is especially apparent for the BDPA sample.

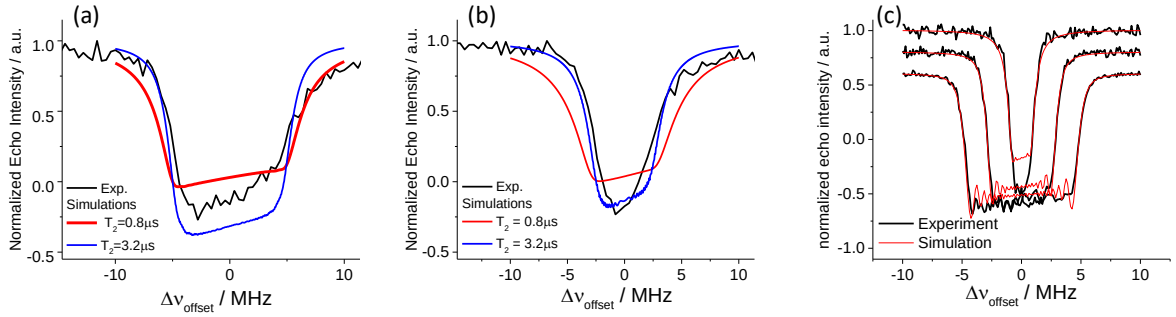

Figure S3. Comparison between the experimental and simulated inversion profiles for diamond sample with $\Delta\nu_{chirp}$ = 10 MHz (a) and $\Delta\nu_{chirp}$ = 5 MHz (b) and BDPA sample with simulated profiles calculated with T_2 = 3.3 μs (c).

Generation of the pre-distorted input waveform based on the measured AMC calibration table

To correct for the imperfections and non-linearity of the AMC output, we developed a procedure for generating the pre-distorted 12 GHz waveform that is sent to the AMC for generating phase and amplitude modulated waveforms at 200 GHz. The algorithm calculates the amplitude and phase of the input waveform for each time step by locating the amplitude and phase of a target 200 GHz waveform in the calibration table (Figure 6d in the main text) and interpolating for the 12 GHz amplitude and phase. To calculate the first point of the corresponding input waveform, the algorithm takes the first point of the 200GHz waveform and looks for a closest match in the lookup table. The x (phase) and y (amplitude) axes corresponding to this point in the lookup table provide the corresponding phase and amplitude for the low frequency input waveform. It is important to note that the x16 frequency multiplication also results in a x16 phase multiplication on the output waveform. This results in 16 equally valid input solutions that generate the phase and amplitude of the target 200 GHz waveform. If we allow an unconstrained search, i.e. the algorithm can return any solution that produces the closest match to the 200 GHz waveform. The algorithm returns a jagged 12 GHz waveform with a phase jumps ≥ π/8, which are due to 16 possible phase solutions for the 12 GHz waveform. The jagged 12 GHz waveform generates significant phase transients at 200 GHz because the 200 GHz phase is instantaneously (~1 ns) changing by ≥ 2π. By constraining the algorithm to only return a solution that is within ± π/16 of the solution for the previous time step we get a solution with a smooth phase for the 12 GHz input waveform. This constraint generates a smooth waveform at 200 GHz and does not impose any constraints on the output waveform in any way.

Theoretical model

In order to have a quantitative benchmark on the performance of the 200GHz AWG spectrometer we compare the experimental results to simulations. The response of the S=1/2 spin system to a phase modulated pulse was simulated, by including the experimental (ω_1) parameter as well as intrinsic relaxation parameters (T_1 and T_2) as described below.

The rotating frame Hamiltonian describing the coherent evolution of the spin system during the phase-modulated pulse is given by:

$$\widehat{H}(t) = \Delta\omega(t)\hat{S}_z + \omega_1\left(\hat{S}_x\cos(\theta(t)) + \hat{S}_y\sin(\theta(t))\right) \quad (5)$$

Where ω_1 is the microwave irradiation frequency strength, $\Delta\omega$ is the off resonance offset and $\theta(t)$ the phase profile of the phase modulated pulse.

The density matrix at equilibrium is given by:

$$\sigma(0) = \frac{e^{-\beta\omega_e S_z}}{tr\left(e^{-\beta\omega_e S_z}\right)} \quad (6)$$

Where ω_e is the electron Larmour frequency, $\beta = \frac{\hbar}{k_b T}$, where $\hbar$ and k_b are Planck and Boltzmann constants and T is the temperature.

To evaluate the spin evolution during the phase modulated pulse, taking relaxation effects into account, we utilize the Liouville superoperator formalism.[27] The density matrix evolution for a time independent Hamiltonian is given by:

$$\frac{d}{dt}\hat{\sigma}(t) = -i\left[\hat{\hat{H}} - \hat{\hat{\Gamma}}\right]\hat{\sigma}(t) \quad (7)$$

where $\hat{\sigma}(t)$ is the 4x1 Liouville space representation of the density matrix at time t; $\hat{\hat{H}}(t)$ is the superoperator form of $\hat{H}(t)$ defined as $\hat{\hat{H}}_{klmn} = \hat{H}_{kl}\delta_{mn} - \hat{H}_{mn}\delta_{kl}$ and $\hat{\hat{\Gamma}}$ is the relaxation matrix defined as

$$\hat{\hat{\Gamma}} = \begin{bmatrix} iR_1 & 0 & 0 & -i\varepsilon R_1 \\ 0 & iR_2 & 0 & 0 \\ 0 & 0 & iR_2 & 0 \\ -iR_1 & 0 & 0 & i\varepsilon R_1 \end{bmatrix} \quad (8)$$

where the longtitudinal and transverse relaxation rates are given by $R_1 = \frac{1}{T_1}$ and $R_2 = \frac{1}{T_2}$ respectively and $\varepsilon = e^{\left(\frac{-g\beta B_0}{k_b T}\right)}$ is the Boltzman factor.

The solution of eq (7) is given by

$$\hat{\sigma}(t) = \hat{\hat{U}}_L(t)\hat{\sigma}(0) \quad (9)$$

Where

$$\hat{\hat{U}}_L(t) = \exp\left(\left[\hat{\hat{H}}(t) - \hat{\hat{\Gamma}}\right]dt\right). \quad (10)$$

It is important to note that the Liouvillian formalism assumes a time-independent Hamiltonian. In this simulation, the only time-dependent term is the ω_1 field which is changing for every AWG step. We thus chose a $dt = 1ns$ time interval that is equal to the AWG time resolution. The calculation is performed sequentially for every step of constant ω_1 in the phase-modulated pulse profile. The final state of the spin system, after the pulse consisting of *N* time steps of length *dt* is given by:

$$\hat{\sigma}(t) = \prod_{L=1}^{N} \hat{\hat{U}}_L(\mathrm{d}t)\hat{\sigma}(0) \quad (11)$$

The simulated inversion profile is thus given by the final magnetization, calculated from density matrix obtained from eq (11), at the end of the pulse for a range of frequency offsets, Δω, that span the range of the inversion pulse frequency spectrum.

The echo shapes were calculated by taking into account an inhomogeneous EPR line shape, with the echo signal given by:

$$\hat{\sigma}(t) = \int \hat{\sigma}(t, \Delta\omega)\mathrm{g}(\Delta\omega)\mathrm{d}\Delta\omega$$

Where $\mathrm{g}(\Delta\omega)$ is an EPR lineshape approximated by a Gaussian distribution with a full width at half maximum of 10 MHz.

Generation of pulse sequences longer than the AWG memory limit.

For some experiments, notably ELDOR and inversion recovery, a need arises to generate pulse sequences that exceed in length the 15us memory limit of our AWG. In the often encountered case where only part of the sequence requires shaped pulses it is possible using our setup to generate longer pulse sequences where part of the sequence (<15us) is generated with AWG and the rest of the pulse sequence is generated using the PB controlled mw switches. Since in our setup there is no fast switch allowing for quick bypass of AWG IQ mixer it is necessary to set AWG board to generate a CW output from the IQ mixer that can be "chopped" later by the PB-controlled mw switches. In order to achieve this our AWG board can be programmed to indefinitely repeat the last four bits of the waveform which are customarily set to full amplitude of the real (I) channel. This concept is illustrated in figure S4. A pulse sequence that exceed the memory of the AWG board is shown on Figure S4b, part of the sequence is generated by the AWG and is shown in blue while for the rest of the sequence AWG output is set to its maximum level. The rest of the sequence (which can consist of only the square pulses) is produced by PB-controlled mw switches is shown in Figure S4d.

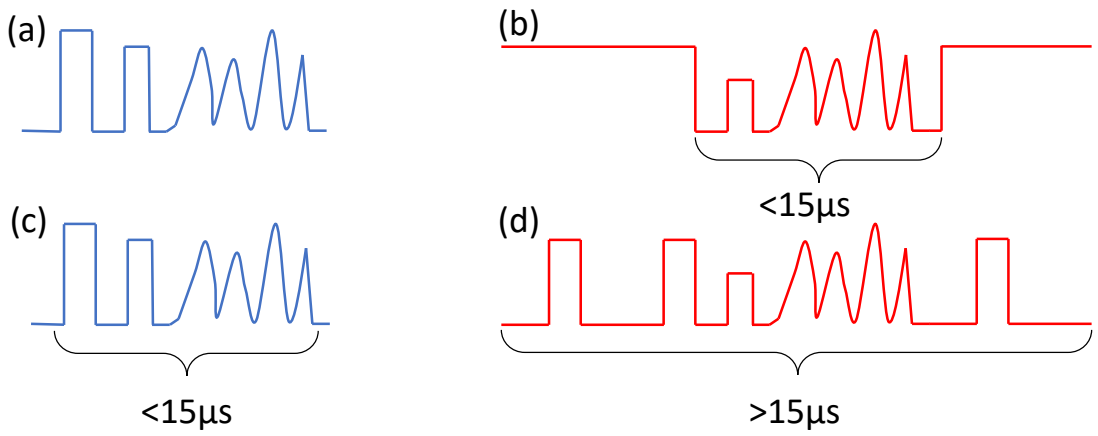

Figure S4. Waveform programmed into the AWG board when short pulse sequence <15k points is required (a) and long >15k points (b). Final waveform after additional pulses are generated by PB controlled switches for the same two cases (c),(d). Note that for short waveforms the two are identical while for long waveforms additional pulses are sliced by PB controlled mw switches from CW mw irradiation synthesized by AWG.